Hindawi
Advances in Civil Engineering
Volume 2024, Article ID 6682882, 12 pages
https://doi.org/10.1155/2024/6682882

Research Article

Slope Stability Analysis of Mounded Storage Tank under Different Compaction Coefficients

Yunsheng Ma,[1] Zizhuo Tao,[2,3] Yu Zhang ,[2,3] Zhenxue Liu,[1] Shengke Wei,[1] and Fenghao Qing [3]

[1]*Chambroad Holding Group, Binzhou 256599, China*
[2]*Key Laboratory of Ministry of Education on Safe Mining of Deep Metal Mines, Northeastern University, Shenyang 110819, China*
[3]*College of Pipeline and Civil Engineering, China University of Petroleum (East China), Qingdao 266580, China*

Correspondence should be addressed to Yu Zhang; zhangyu@upc.edu.cn and Fenghao Qing; z21060144@s.upc.edu.cn

Received 26 June 2023; Revised 24 December 2023; Accepted 17 January 2024; Published 13 February 2024

Academic Editor: Jianyong Han

Mounded storage tank is to cover the storage tank with compacted soil on the ground to avoid steam cloud explosion, ensuring the stability and safety of the storage tank. In view of the influence of large diameter and surface radian of the tank, slope stability of mounded storage tank under different compaction coefficients has become the focus of research. In this paper, a series of laboratory tests were carried out to obtain the physical and mechanical parameters of the soil samples collected from the overburden of one specific engineering project. On this basis, Plaxis2D finite element software was used to establish a numerical model of the horizontal tank with a diameter of 7.6 m and a length of 76 m and the mounded slope with a height of 16.25 m as the research object. The effects of different compaction coefficients, slope angles, and overburden thicknesses on the slope stability of the mounded storage tank are investigated. Results indicate that the slope stability coefficients increase with the increase of compaction coefficient but decrease with the increase of slope angle and overburden thickness. Under the condition of the compaction coefficient 0.75–0.95, slope angle 30°–60°, and overburden thickness 0.5–1.3 m, the sensitivity ranking on the slope stability of mounded storage tank is: compaction coefficient, slope angle, and overburden thickness. The analysis results can provide an important theoretical basis and technical support for the safety and stability evaluation of mounded horizontal tank project.

1. Introduction

Hazardous chemical storage tanks are often used to store flammable and explosive, toxic, and highly corrosive gases or liquids, which are prone to fire, explosion, and other major hazardous accidents, causing environmental pollution and casualties. Therefore, it is very important to ensure the safety and stability of hazardous chemical storage tanks. Mounded storage tank is a new type of protection technology for hazardous chemicals facilities conforming to the concept of green environmental protection, energy conservation, and carbon reduction in current chemical industries. It uses compacted soil to cover the tank on the ground (Figure 1), forming a protective layer around the tank to avoid steam cloud explosions and protect the tank from damage by other dangerous sources such as nearby heat sources, explosion shock waves, and splashing objects, essentially playing the role of safety protection for the storage tanks [1–3]. Given the importance of hazardous chemicals storage tanks to people's safety, slope stability of mounded storage tank is the focus of tank research. However, China's mounded storage tank technology is still in its infancy, and there is no relevant specification standard. Therefore, a study on the slope stability of mounded storage tank was carried out in this paper.

The technology of mounded storage tank originated in Germany and has been widely used in France, Japan, Taiwan, China, South Africa, India, and other countries [4], but it is still in its infancy in China. Jing-bo [5] analyzed that mounded storage tank can improve storage safety, reduce construction cost, save floor area, and reduce safety distance with surrounding adjacent facilities when compared to above-ground spherical tank; Mishael and Shenoi [6], Kumar and Kumar

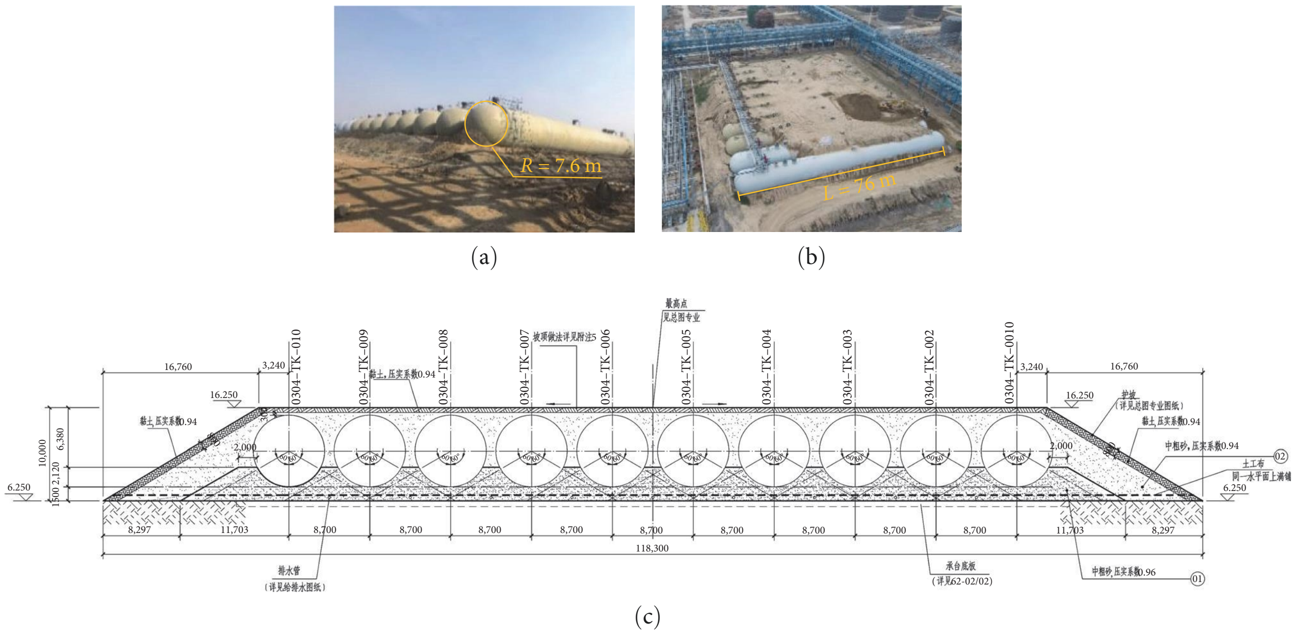

Figure 1: Mounded storage tank: (a) entity side view; (b) entity top view; and (c) construction profile.

[7], Yogesh and Lakshmi [8], and Guo-qiang and Jin-xiang [9] used finite element technology to simulate the stress analysis under design conditions, seismic conditions, and hydrostatic test conditions based on the EEMUA 190 international guide [3]. The EEMUA 190 international guide states a minimum compaction coefficient of 0.95 and a minimum overburden thickness of 0.5 m. The slope stability of mounded storage tank is the key for ensuring the intrinsic safety of the tank. At present, most existing domestic research refers to the stability analysis method of homogeneous soil to study the mounded storage tank. Lichun et al. [10] analyzed the slope stability under different slope angles and slope forms; Peng et al. [11] compared the influence of soil elastic modulus and internal friction angle on the sliding and cracking law of mounded tank slope; Yuan et al. [12, 13] proposed that polymer SH and glass fibers can increase the impact resistance of soil, alkaline solution, and fibers to enhance the increase in soil compression; Bai et al. [14] developed a granular thermodynamic compression theory in view of the soil particle rearrangement; Linwan et al. [15] combined macro-, fine-, and microscopic studies of compacted loess and found that an increase in the compaction of filler can improve the strength of the soil; Ze-ying [16] proposed an empirical formula for the calculation of slope stability coefficient and investigated the influence of internal friction angle, cohesion, soil weight, slope height, and slope angle on slope stability coefficient. Existing research mainly focused on the design and finite element simulation of storage tanks under operation conditions. Few studies have been reported on the slope stability of mounded storage tanks under different compaction coefficients.

In this paper, based on laboratory tests, Plaxis2D software is applied to simulate the slope stability of mounded storage tanks under different compaction coefficients, slope angles, and overburden thicknesses to provide a significant theoretical basis and technical support for the safety and stability of mounded storage tank project.

2. Physical and Mechanical Parameters of Soil

A Chinese group is proposing to perform the construction of the world's largest mounded horizontal tank in China to date, with a length of 80.5 m, a diameter of 7.7 m, and a volume of 3,300 m^3. The total height is 16.25 m, and the total area of the project is 12,000 m^2. Taking this project as the engineering background, soil samples were obtained on-site to conduct geotechnical tests to measure the basic physical and mechanical parameters.

2.1. Soil Parameters. The maximum dry density and the optimum moisture content of the soil samples are measured by compaction tests. The relationship curve between five different moisture contents and dry densities is shown in Figure 2. The vertical and horizontal coordinates corresponding to the peak point of the curve are the maximum dry density and the optimum moisture content of the soil. The maximum dry density of the soil sample is 1.90 g/cm^3, and the optimum moisture content is 15.1%.

Particle size analysis of the undisturbed soil samples was carried out using the screening method. The total weight of the dried samples before the test was 500 g. The total weight after sieving is 499.6 g, and the loss rate after sieving is 0.08%. The result of the sieving test is presented in Table 1, and the particle size distribution curve is shown in Figure 3.

2.2. Mechanical Parameters. Direct shear tests are commonly used to measure the shear strength of soil samples at different pressures. Soil samples with compaction coefficients of

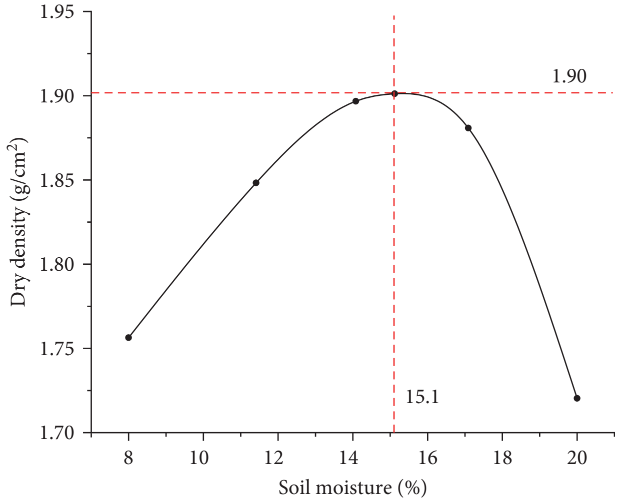

FIGURE 2: The relationship curve between soil moisture and dry density.

TABLE 1: Sieving test results.

Sieve size (mm)	Mass of retained soil (g)	Percentage of passing (%)
5	17.7	96.46
2	180.9	60.28
1	52.1	49.86
0.5	61.9	37.48
0.25	40.2	29.44
0.075	29	23.64
0	117.8	0.08

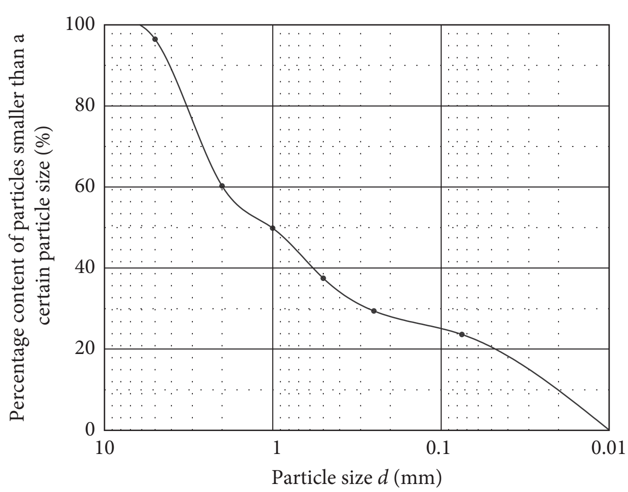

FIGURE 3: The particle size distribution curve.

0.75, 0.80, 0.85, 0.90, and 0.95 were prepared by controlling the sample quality: The dry density of the sample was obtained from the specified compaction coefficient, and the measured maximum dry density and the required mass of water and dry soil was calculated based on the fixed volume of the container. The normal pressure applied during the test is 100, 200, 300, and 400 kPa, respectively. The displacement rate of the shear test is designated as 6 cycles/min. The results of the direct shear tests are shown in Table 2.

The fitted curves of the direct shear tests under compaction coefficients were obtained through linear regression analysis. The internal friction angle, φ and the cohesion force, c were determined according to the slope and intercept of the fitting line, as shown in Table 3.

3. Stability of Storage Tank Soil Slope

3.1. Numerical Model. Compared with other numerical simulation software, Plaxis2D is easy to operate in dealing with slope stability analysis, having more stable calculation process and credible simulation results. In this paper, a numerical model is developed using finite element software Plaxis2D to simulate the construction process of the mounded storage tank. The impacts of different compaction coefficients, slope angles, and overburden thicknesses on the slope stability of the mounded storage tank are analyzed. To meet the requirements of numerical modeling and ensure that there is no excessive deviation from the actual situation, the following assumptions are proposed:

(1) The whole model is axisymmetric. To simplify the calculation process, only the left mounded storage tank is taken for numerical modeling and analysis;

(2) The foundation, the soil on the right side of the tank, and the tank are all set as rigid materials, which do not affect the strength of the surrounding soil since they are not the focus of this study;

(3) Although moisture content and water infiltration cannot be ignored [17], due to waterproofing treatment on site, the influence of moisture content change on slope stability is not considered. The soil is kept at the optimal moisture content of 15.1%;

(4) According to the site construction steps, the phased construction is divided into: excavation (gravity loading), sand bed construction, soil construction, and strength reduction method to calculate the slope stability coefficient.

The main parameters of the numerical simulation are shown in Table 4.

The numerical model is established and the cells are divided, as shown in Figure 4 (contains 1,217 generated units and 9,461 nodes). Mohr–Coulomb material ontology model is selected for the soil material in "Soils and Sections." The entire model takes the site mounded storage tank as a reference with a tank radius of 3.825 m and a height of 1.5 m from the bottom of the tank to the foundation. The right side of the tank is 1 m away from the rigid material boundary, and the height of the sand bed is 3.412 m (the sand bed is at 120° of the tank). Horizontal displacement of the nodes on both sides of the model is constrained, the displacement of the bottom node is completely constrained, and the top node

Table 2: Direct shear test results.

Normal pressure (kPa)	Shear strength (kPa)				
	0.75 Compaction	0.80 Compaction	0.85 Compaction	0.90 Compaction	0.90 Compaction
100	53.233	57.176	68.184	79.192	94.965
200	101.87	108.44	120.76	134.72	150.17
300	156.08	166.27	176.13	189.27	202.09
400	205.38	216.88	238.24	253.02	261.57

Table 3: Shear strength coefficient at different compaction.

Compaction coefficient	0.75	0.8	0.85	0.9	0.95
Cohesion force, c (kPa)	1.47	2.95	9.44	20.04	39.26
Internal friction angle, φ (°)	27.04	28.23	29.48	29.94	28.88

Table 4: Numerical simulation parameters.

Parameter	0.75 Compaction	0.80 Compaction	0.85 Compaction	0.90 Compaction	0.95 Compaction	Foundation	Sand bed
Elastic modulus (GP)	30E3	30E3	30E3	30E3	40E3	200E9	40E3
Poisson's ratio	0.35	0.35	0.35	0.35	0.35	0.3	0.35
Dry weight (kN/m^3)	14.25	15.20	16.12	17.10	18.05	70	18.05
Saturation weight (kN/m^3)	21.90	21.90	21.90	21.90	21.90	70	21.90
Cohesion force (kPa)	1.497	2.957	9.447	20.05	39.27	—	39.27
Internal friction angle (°)	27.05	28.23	29.49	29.94	28.89	—	28.89

Note. The dry weight is calculated from maximum dry weight and compaction; saturated weight, elastic modulus, Poisson's ratio can be obtained according to the assumptions of Section II and the common range of values; shear strength can be obtained from Section II.

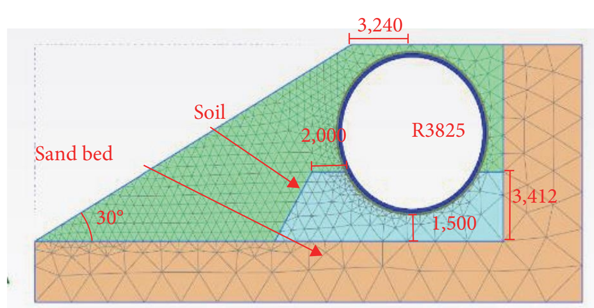

Figure 4: Plaxis2D calculation model and cell division (unit: mm).

is unconstrained. During the numerical simulation, the strength parameters of the slope are continually reduced based on the Mohr–Coulomb criterion until converge to determine the slope stability coefficient (through the final step of phased construction, with safety selected for calculation type and displacement reset to 0). This numerical simulation controls the compaction coefficient by changing the soil parameters (physical parameter: heaviness and mechanical parameter: shear strength). The slope angle is controlled by changing the slope angle on the left side of the model and keeping the right side unchanged. The overburden thickness is controlled by changing the height of the soil layer, keeping the length of the topsoil unchanged, and moving the slope to the left, respectively. The effects of the three influencing factors on slope stability are analyzed.

3.2. Result Analysis. Plaxis2D uses the strength reduction method to calculate the slope stability coefficient. The reduction processes of slope stability coefficients under different compaction coefficients, slope angles, and overburden thicknesses are shown in Figures 5–9 (the simulation result of stability coefficient <1 cannot be constructed) and the results are shown in Tables 5–7.

As shown in Figure 10, the stability coefficient of the whole tank slope is >1 when the slope angle is 30°. However, according to GB50330-2013 *Technical Code for Building*

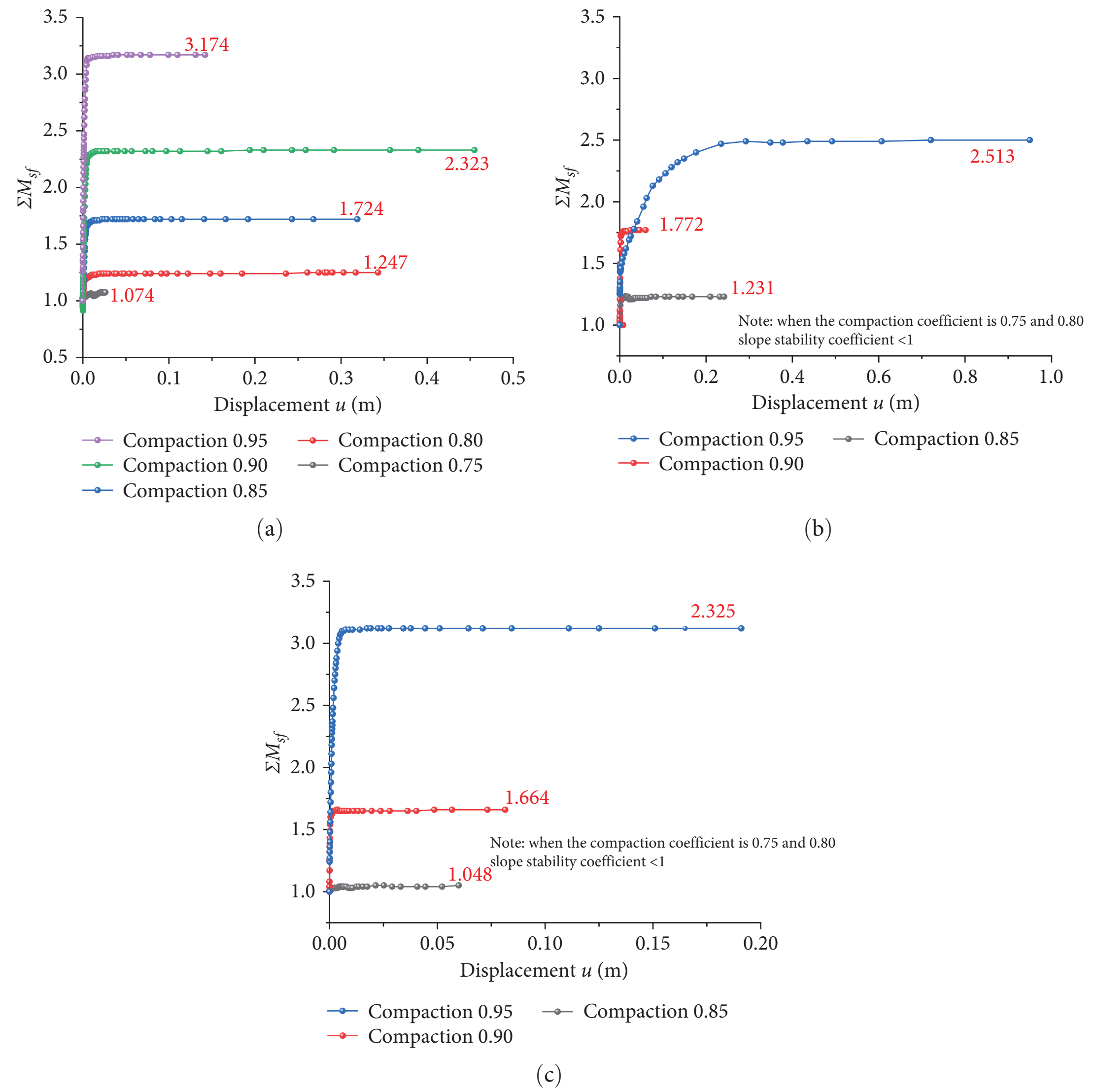

Figure 5: Reduction process of stability coefficient of overburden thickness 0.5 m: (a) broken angle 3°; (b) broken angle 45°; and (c) broken angle 60°.

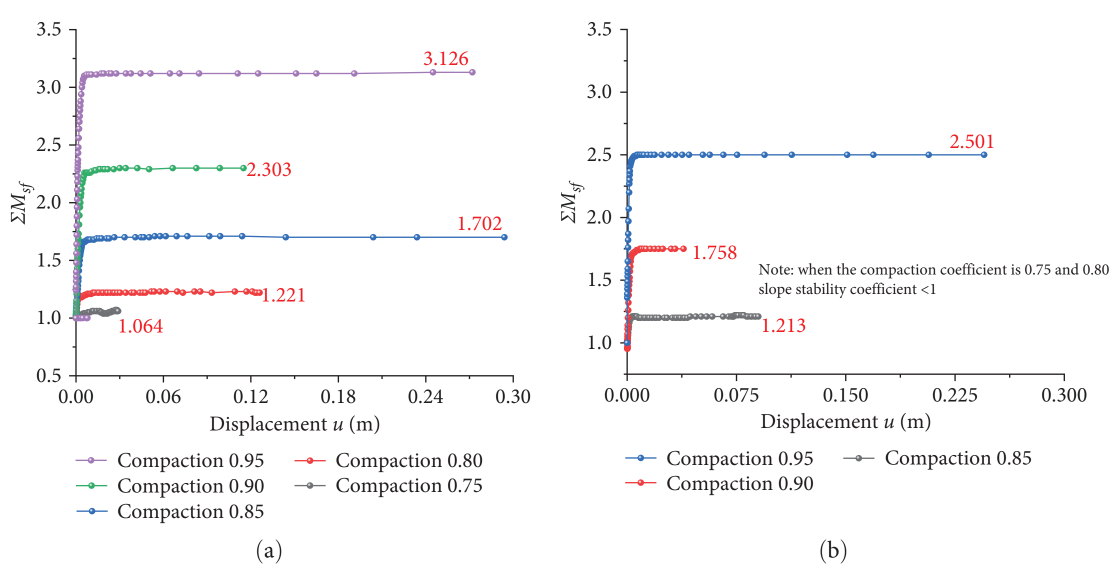

Figure 6: Continued.

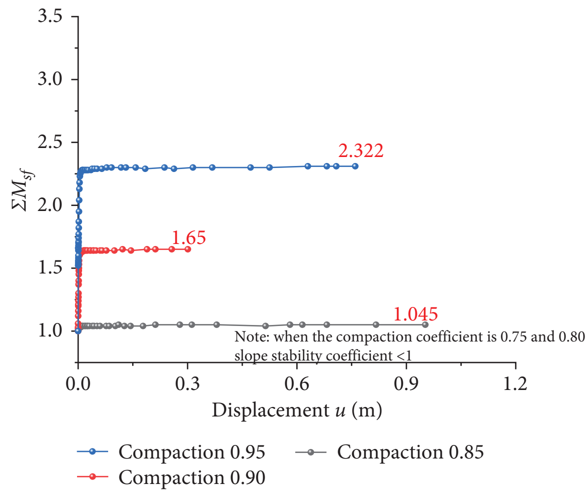

(c)

Figure 6: Reduction process of stability coefficient of overburden thickness 0.7 m: (a) broken angle 3°; (b) broken angle 45°; and (c) broken angle 60°.

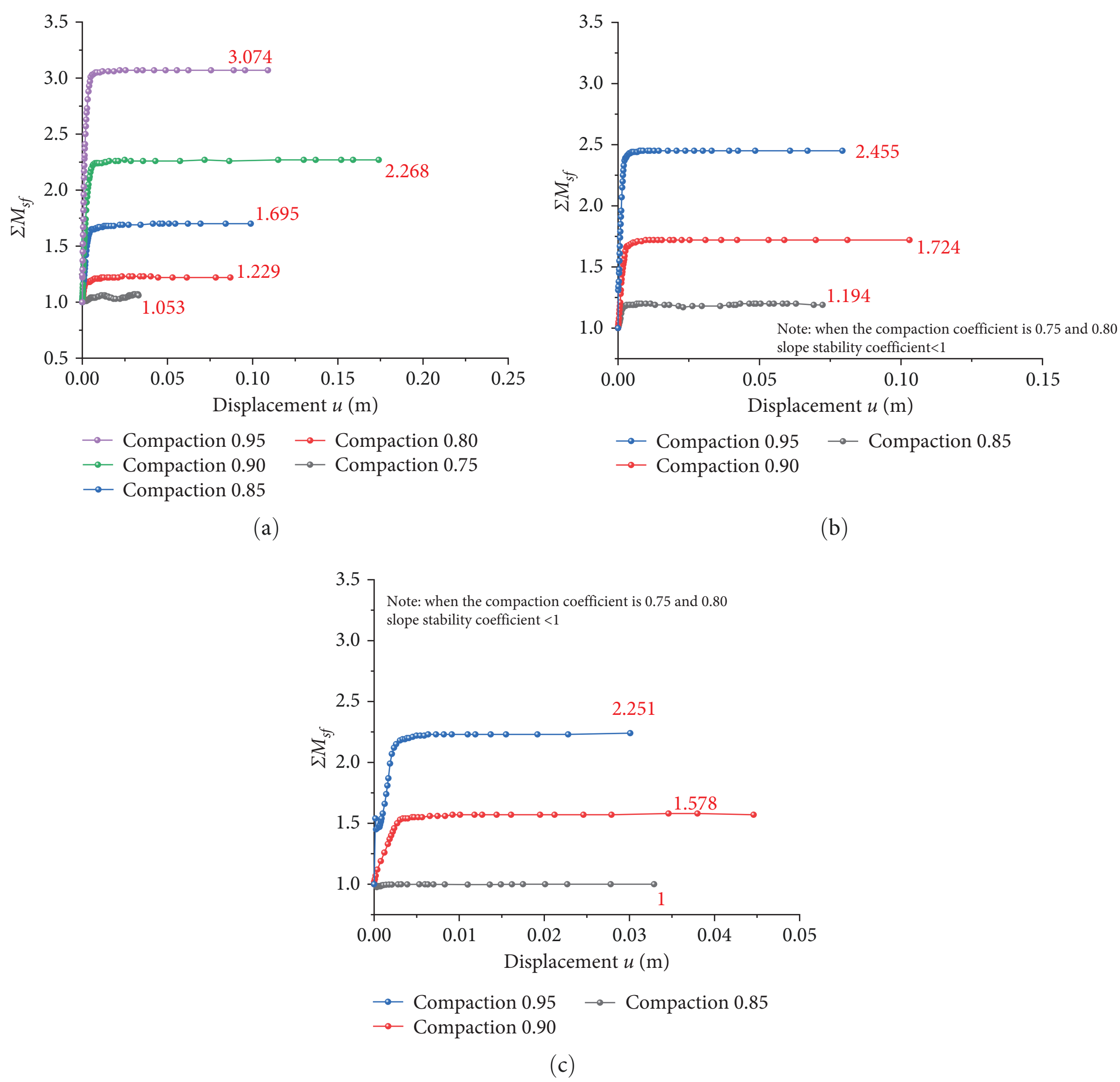

Figure 7: Reduction process of stability coefficient of overburden thickness 0.9 m: (a) broken angle 3°; (b) broken angle 45°; and (c) broken angle 60°.

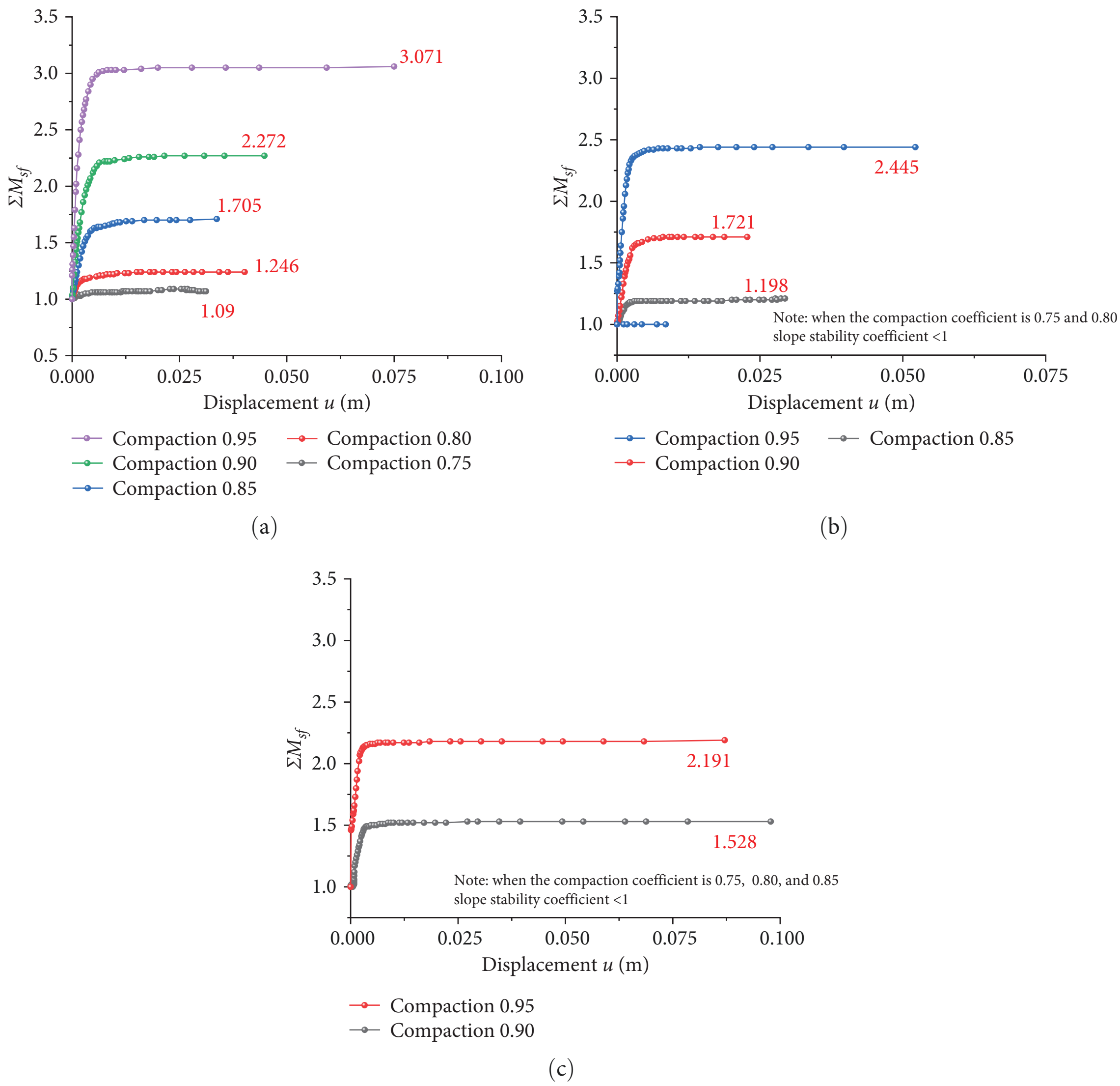

Figure 8: Reduction process of stability coefficient of overburden thickness 1.1 m: (a) broken angle 3°; (b) broken angle 45°; and (c) Broken angle 60°.

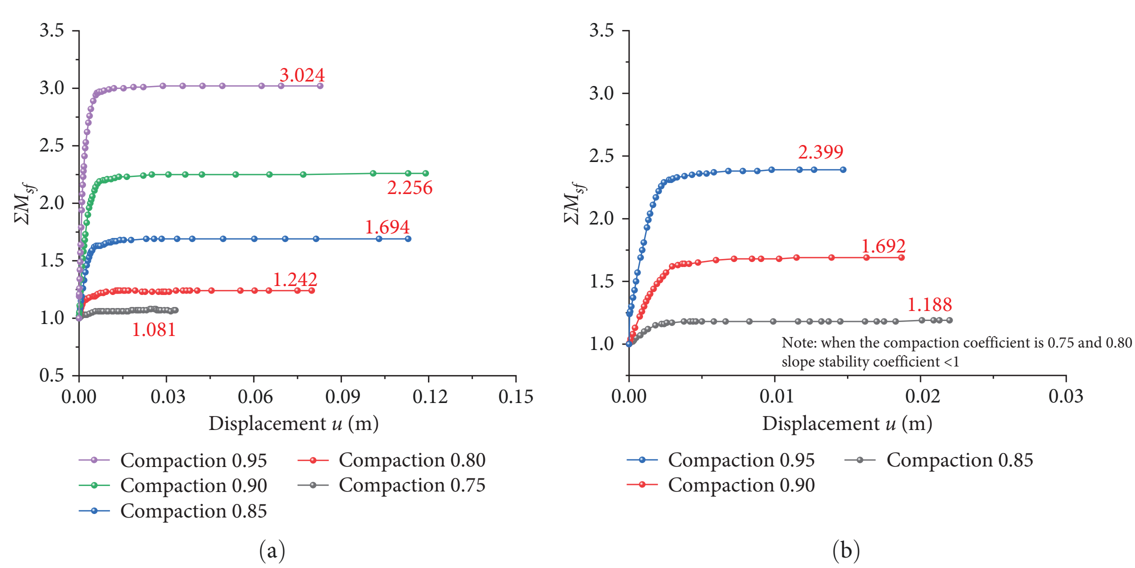

Figure 9: Continued.

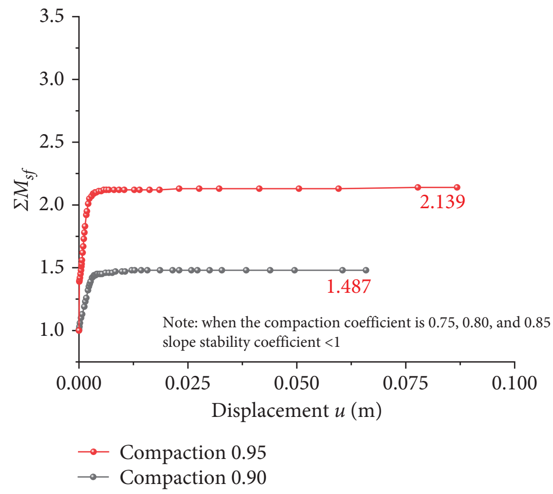

(c)

Figure 9: Reduction process of stability coefficient of overburden thickness 1.3 m: (a) broken angle 3°; (b) broken angle 45°; and (c) broken angle 60°.

Table 5: Slope angle 30° stability coefficient.

Overburden thickness (m)	Slope stability coefficient (K)				
	0.75 Compaction	0.80 Compaction	0.85 Compaction	0.90 Compaction	0.95 Compaction
0.5	1.074	1.247	1.724	2.323	3.174
0.7	1.064	1.221	1.702	2.303	3.126
0.9	1.053	1.229	1.695	2.268	3.074
1.1	1.09	1.246	1.705	2.272	3.071
1.3	1.081	1.242	1.694	2.256	3.024

Table 6: Slope angle 45° stability coefficient.

Overburden thickness (m)	Slope stability coefficient (K)				
	0.75 Compaction	0.80 Compaction	0.85 Compaction	0.90 Compaction	0.95 Compaction
0.5	<1	<1	1.231	1.772	2.513
0.7	<1	<1	1.213	1.758	2.501
0.9	<1	<1	1.194	1.724	2.455
1.1	<1	<1	1.198	1.721	2.445
1.3	<1	<1	1.188	1.692	2.399

Table 7: Slope angle 60° stability coefficient.

Overburden thickness (m)	Slope stability coefficient (K)				
	0.75 Compaction	0.80 Compaction	0.85 Compaction	0.90 Compaction	0.95 Compaction
0.5	<1	<1	1.048	1.664	2.325
0.7	<1	<1	1.045	1.65	2.322
0.9	<1	<1	1	1.578	2.251
1.1	<1	<1	<1	1.528	2.191
1.3	<1	<1	<1	1.487	2.139

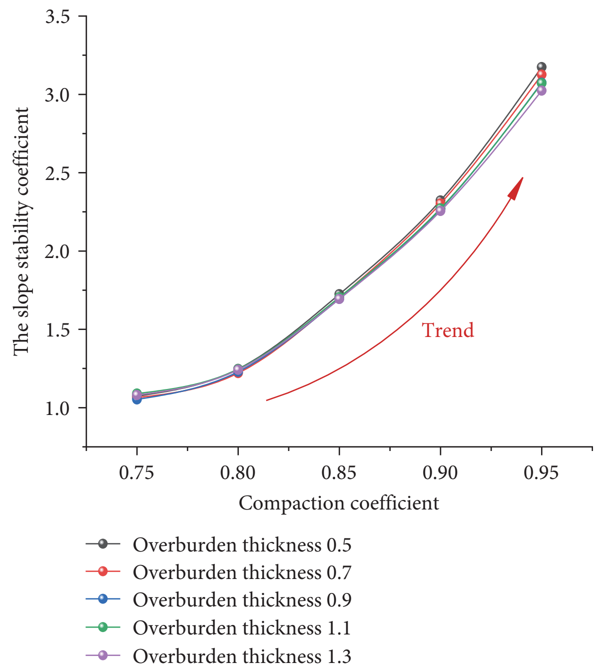

FIGURE 10: Slope stability coefficient with slope angle of 30°.

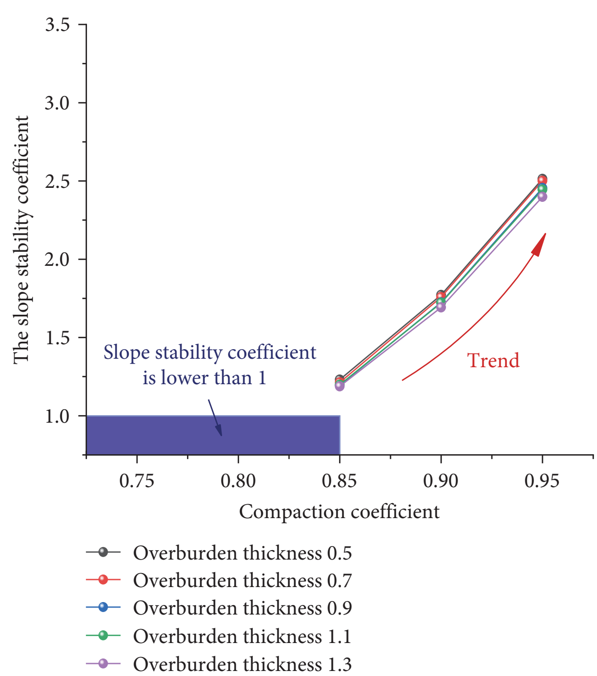

FIGURE 11: Slope stability coefficient with slope angle of 45°.

Slope Engineering, the slope stability coefficient is <1.25 when the compaction coefficient is 0.75 and 0.8, which cannot meet the requirements of the slope stability coefficient of Grade III safety level, and the slope needs to be reinforced. The slope stability coefficient gradually increases with the increase of the compaction coefficient, reaching 3.174 when the overburden thickness is 0.5 m and the compaction coefficient is 0.95.

When the slope angle is 45°, as shown in Figure 11, the slope stability coefficient is <1 when the compaction coefficient is 0.75 and 0.80, which is unstable. When the compaction coefficient is 0.85, the slope stability coefficient is <1.25, and the slope should be reinforced. The slope stability coefficient gradually increases with compaction coefficient, and the maximum stability coefficient reaches 2.513 when the overburden thickness is 0.5 m and the compaction coefficient is 0.95.

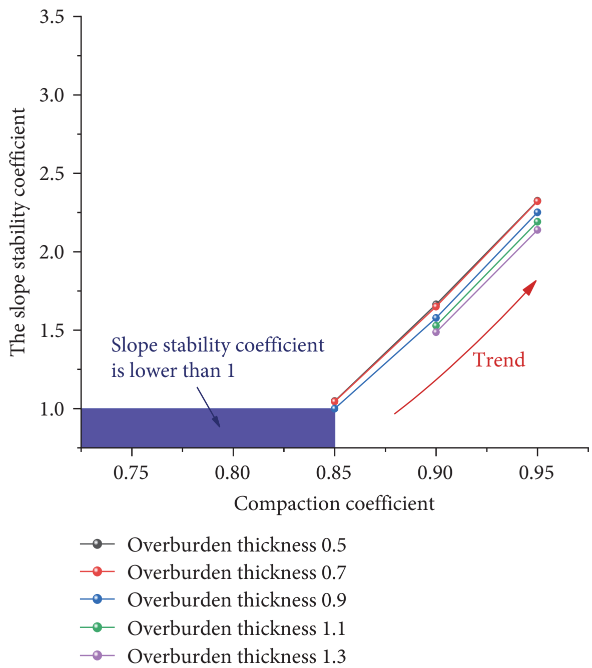

FIGURE 12: Slope stability coefficient with slope angle of 60°.

When the slope angle is 60°, as shown in Figure 12, the slope stability coefficient is <1 when the compaction coefficient is 0.75 and 0.80, which is unstable. When the compaction coefficient is 0.85, the slope stability coefficient is <1.25, and the slope should be reinforced. With the increase of compaction coefficient, the slope stability coefficient gradually increases, and the maximum stability coefficient is 2.325 when the overburden thickness is 0.5 m and the compaction coefficient is 0.95.

In summary, it can be seen that when the angle of the slope is 30°, the compaction coefficient must reach 0.85 to meet the construction requirements. When the slope angle is 45° and 60°, respectively, the compaction coefficient of the slope must reach 0.9 to meet the construction requirements, otherwise the slope should be reinforced. In addition, with the increase of compaction coefficient, the soil is compacted, the shear strength of the soil increases, and the slip resistance of the sliding surface of the slope increases, resulting in the increase of the slope stability coefficient. It can be inferred from the data summarized in Tables 5–7 that as the slope angle increases, the required slip resistance of the slope increases, the slope stability decreases, and the slope stability coefficient continues to decrease; as the overburden thickness increases, the slope stability coefficient slowly decreases. However, when the slope angle is at 30° and the compaction coefficient is at 0.75–0.90, and when the slope angle is at 45° and the compaction coefficient is at 0.85, an increase in the stability coefficient occurs when the overburden thickness is at 1.1 m. The possible causes are analyzed as follows:

The displacement cloud of the mounded storage tank with a 30° slope angle and 0.7 m overburden thickness in the calculation of the slope stability coefficient is shown in Figure 13. Although the stability coefficient increases with the increase in compaction coefficient, the landslide area is also increasing, becoming more tangent to the tank. The displacement cloud of the tank with a 30° slope angle and 0.85 compaction coefficient is shown in Figure 14, the landslide area remains essentially constant and tangent to the tank. The increase in overburden thickness leads to a slight upward movement of the sliding surface, which is no longer tangent to the tank at the overburden thickness of 1.1 m, improving the slope stability coefficient.

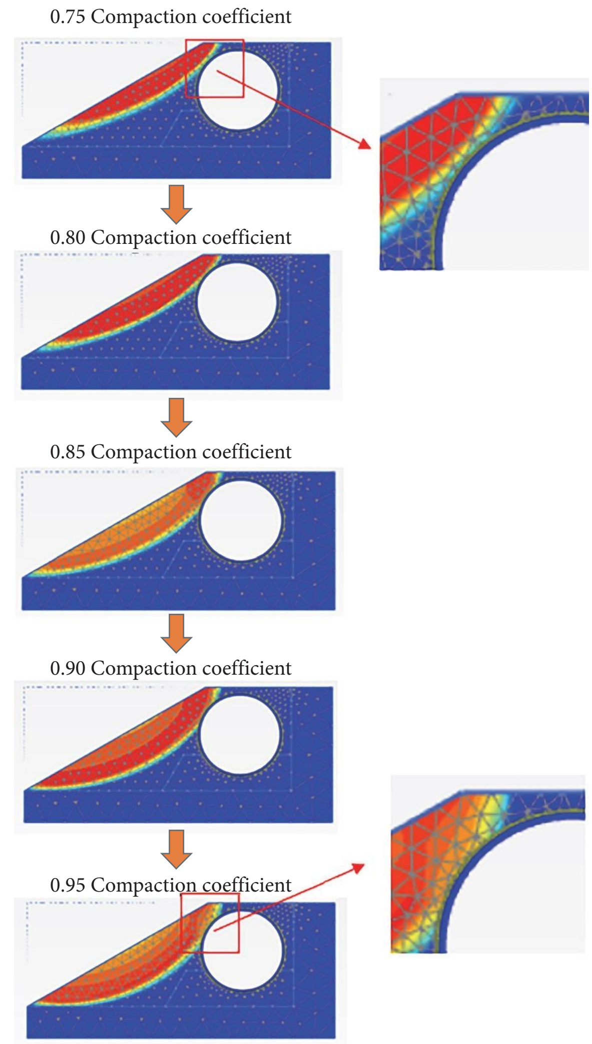

FIGURE 13: Displacement cloud for 30° slope angle and 0.7 m overburden thickness.

3.3. Sensitivity Analysis. The overburden thickness of 0.5 m, slope angle of 30°, and compaction coefficient of 0.9 are selected as the basis. The single-factor sensitivity analysis method [18, 19] is applied to simulate the influence of single-factor variation on slope stability while keeping other influencing factors constant. The ratio of the stability factor F and its relative change rate under different factors is calculated and compared as the sensitivity S of each factor, and the larger the ratio represented the greater the influence of the factor on the slope stability. The calculation formula is as follows:

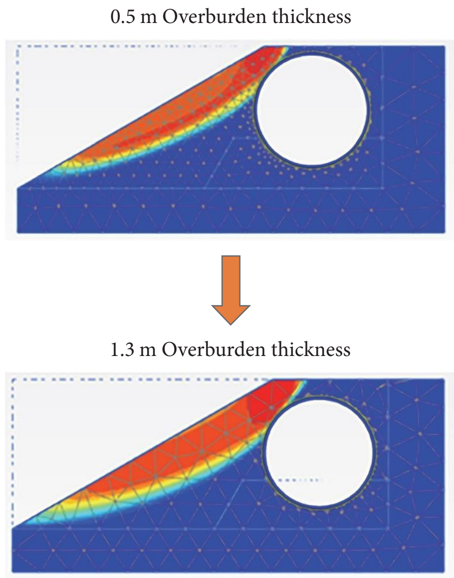

FIGURE 14: Displacement cloud for 30° slope angle and 0.85 compaction coefficient.

TABLE 8: Sensitivity analysis results.

Influence factor	$\|\Delta F_i/F_i\|$	$\|\Delta X_i/X_i\|$	S_i
Compaction coefficient	0.662	0.211	3.137
Slope angle	0.267	1	0.267
Covering soil thickness	0.047	1.6	0.029

$$S_i = \frac{|\Delta F_i/F_i|}{|\Delta X_i/X_i|}. \tag{1}$$

where X_i is the influencing factor; F_i is the stability coefficient; and S_i is the sensitivity of each influencing factor. The results of the sensitivity analysis are shown in Table 8:

When the compaction coefficient is 0.75–0.95, the slope angle is 30°–60°, and the overburden thickness is 0.5–1.3 m, the sensitivity of the factors influencing the slope stability of the mounded storage tank in descending order is compaction coefficient, slope angle, and overburden thickness.

4. Conclusions

In this paper, numerical simulation stability analysis of the slope of the mounded storage tank was carried out using the finite element software Plaxis2D based on the physical and mechanical tests of the in-situ soil. The major conclusions are as follows:

(1) To meet the construction requirements of the mounded storage tank, when the slope angle is 30°, the compaction coefficient should reach 0.85 or above. When the slope angle of the storage tank is 45° and 60°, the compaction coefficient should reach 0.9 or above;

(2) The slope stability coefficient increases with increasing compaction coefficient, decreases with increasing slope angle, and decreases with increasing overburden thickness;

(3) The sensitivity of the factors influencing the slope stability of the mounded storage tank in descending order is compaction coefficient, slope angle, and overburden thickness.

The results of this paper can provide a theoretical basis for the slope stability analysis and evaluation of mounded storage tanks.

Data Availability

The data generated or used during the study are included within the article.

Conflicts of Interest

The authors declare that they have no conflicts of interest regarding the publication of this paper.

Acknowledgments

This work was supported by funding from the Natural Science Foundation of Shandong Province (no. ZR2019MEE001), National Natural Science Foundation of China (nos. 51890914 and 52179119).

References

[1] X. Wei, “Design and application of mounded storage tank for pressurized storage of liquefied hydrocarbon at ambient temperature,” *Petroleum Engineering Construction*, vol. 44, no. 3, pp. 1–6, 2018.

[2] J. Shan, “Study and simulation analysis of design technology for large-scale horizontal LPG mounded pressure storage tank,” *Chemical Engineering of Oil and Gas*, vol. 49, no. 3, pp. 53–60, 2020.

[3] EEMUA, “Guide for the design, construction and use of mounded horizontal cylindrical vessels for pressurized storage of LPG at ambient temperatures,” 2017.

[4] W. Hui-qin, “Discussion of safety technology and application outlook of earth-covered tank for liquefied hydrocarbons,” *Petrochemical Safety and Environmental Protection Technology*, vol. 4, 2012.

[5] C. ing-bo, “Liquefied hydrocarbon tank arrangement style in ambient temperature and fire prevention measures,” *Guangzhou Chemical Industry*, vol. 41, no. 8, pp. 164–166, 2013.

[6] J. Mishael and V. S. Shenoi, “Design and structural analysis of mounded LPG bullet,” *Esrsa Publications*, vol. 1, 2015.

[7] M. Kumar and C. Kumar, “Finite element analysis on mounded LPG bullets,” *Imperial Journal of Interdisciplinary Research*, vol. 2, no. 11, pp. 466–471, 2016.

[8] K. Yogesh and M. Lakshmi, “Design and finite element analysis of mounded bullet,” *Journal of Exclusive Management Science*, vol. 1, no. 9, 2012.

[9] Y. Guo-qiang and H. Jin-xiang, “Finite element analysis and design of mounded LPG bullet based on ansys/workbench,” *Pressure Vessel Technology*, vol. 35, no. 6, pp. 36–45, 2018.

[10] Z. Lichun, L. Yongjie, Z. He, X. Yongchao, W. Bo, and Q. Limin, "Study on different slope shapes and stability under same slope angle," *China Safety Science Journal*, vol. 32, no. S1, pp. 140–144, 2022.

[11] Y. Peng, H. Qing-shuo, Y. Jia-lin, W. Xiang-nan, and Y. Yu-zhen, "XFEM-based investigation on sliding regularities of soil slopes," *Chinese Journal of Geotechnical Engineering*, vol. 44, no. 8, pp. 1416–1424, 2022.

[12] B. Yuan, W. Chen, Z. Li et al., "Sustainability of the polymer SH reinforced recycled granite residual soil: properties, physicochemical mechanism, and applications," *Journal of Soils and Sediments*, vol. 23, pp. 246–262, 2023.

[13] B. Yuan, W. Chen, J. Zhao et al., "Addition of alkaline solutions and fibers for the reinforcement of kaolinite-containing granite residual soil," *Applied Clay Science*, vol. 228, Article ID 106644, 2022.

[14] B. Bai, R. Zhou, G. Cai, W. Hu, and G. Yang, "Coupled thermo-hydro-mechanical mechanism in view of the soil particle rearrangement of granular thermodynamics," *Computers and Geotechnics*, vol. 137, no. 8, Article ID 104272, 2021.

[15] C. Linwan, Z. Xiaochao, and F. Shan, "Influence of compactness on deformation and failure characteristics of loess filling slope andmicro and micro experimental study," *Science Technology and Engineering*, vol. 22, no. 21, pp. 9274–9280, 2022.

[16] L. Ze-ying, *Large Deformation Finite Element Analysis on the Stability and the Failure Mode of Soil Slope*, Taiyuan University of Technology, 2021.

[17] B. Bai, S. Jiang, L. Liu, X. Li, and H. Wu, "The transport of silica powders and lead ions under unsteady flow and variable injection concentrations," *Powder Technology*, vol. 387, pp. 22–30, 2021.

[18] H. Zhi-xin, "A sensitivity study of influencing factors of covering karst collapse on orthogonal analysis," *China Manganese Industry*, vol. 38, no. 4, pp. 81–85, 2020.

[19] J. Juan, S. Linhui, and F. Qinshan, "Sensitivity analysis of slope surface damage," *Safety in Coal Mines*, vol. 46, no. 1, pp. 186–189, 2015.